Supporting Information

Highly Active and Stable $Co(Co_3O_4)/Sm_2O_3$ Nano crystallites Derived from Sm_2Co_7 and $SmCo_5$ Intermetallic Compound in NH_3 Synthesis and CO_2 Conversion

Vijaykumar S Marakatti,[a*] Maria Ronda-Lloret,[b] M. Krajčí,[c] Boby Joseph,[d] Carlo Marini,[e] Juan Jose Delgado,[f] François Devred,[a] N. Raveendran Shiju,[b] Eric M Gaigneaux[a*]

[a]*Institute of Condensed Matter and Nanosciences (IMCN), Molecular chemistry, Solids and caTalysis (MOST), Université catholique de Louvain (UCLouvain), Place Louis Pasteur, B-1348 Louvain-la-Neuve, Belgium.*

[b] *Van't Hoff Institute for Molecular Sciences, University of Amsterdam, Science Park 904, Amsterdam 1090 GD, The Netherlands.*

[c] *Institute of Physics, Slovak Academy of Sciences, Bratislava SK-84511, Slovakia*

[d]*Elettra-Sincrotrone Trieste S. C. p. A., S.S. 14, Km 163.5 in Area Science Park, Basovizza 34149, Italy*

[e]*ALBA Synchrotron Light Source, Carrer de la Llum 2-26, Cerdanyola del Vallès, Barcelona, Spain*

[f]*Departamento de Ciencia de los Materiales e Ingeniería Metalúrgica y Química Inorgánica, e IMEYMAT, Instituto Universitario de Investigación en Microscopía Electrónica y Materiales, Universidad de Cádiz, Puerto Real 11510, Spain*

**Corresponding author: eric.gaigneaux@uclouvain.be, chmvijay@gmail.com*

Phone: +32 (0)10 47 36 65 - Fax: +32 (0)10 47 36 49

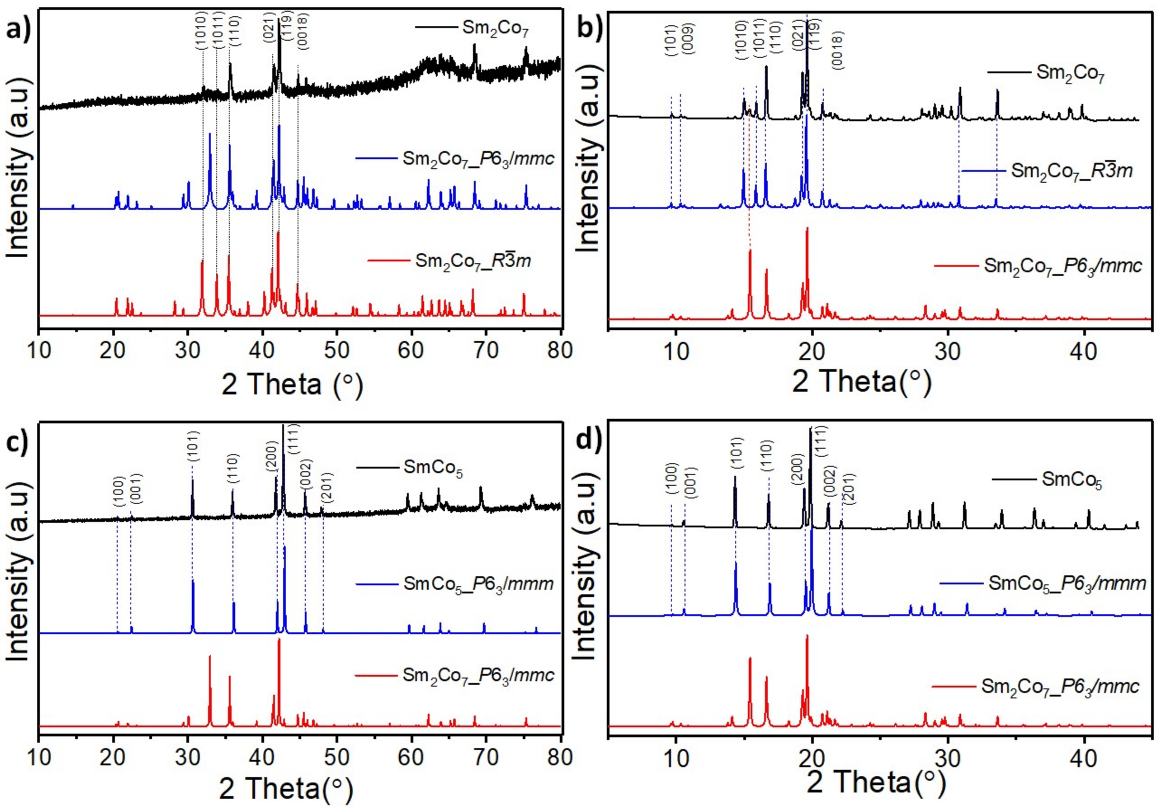

Figure S1. Comparison of low and high energy XRD patterns of Sm_2Co_7(a&b) and $SmCo_5$(c&d) intermetallic compounds with simulated patterns

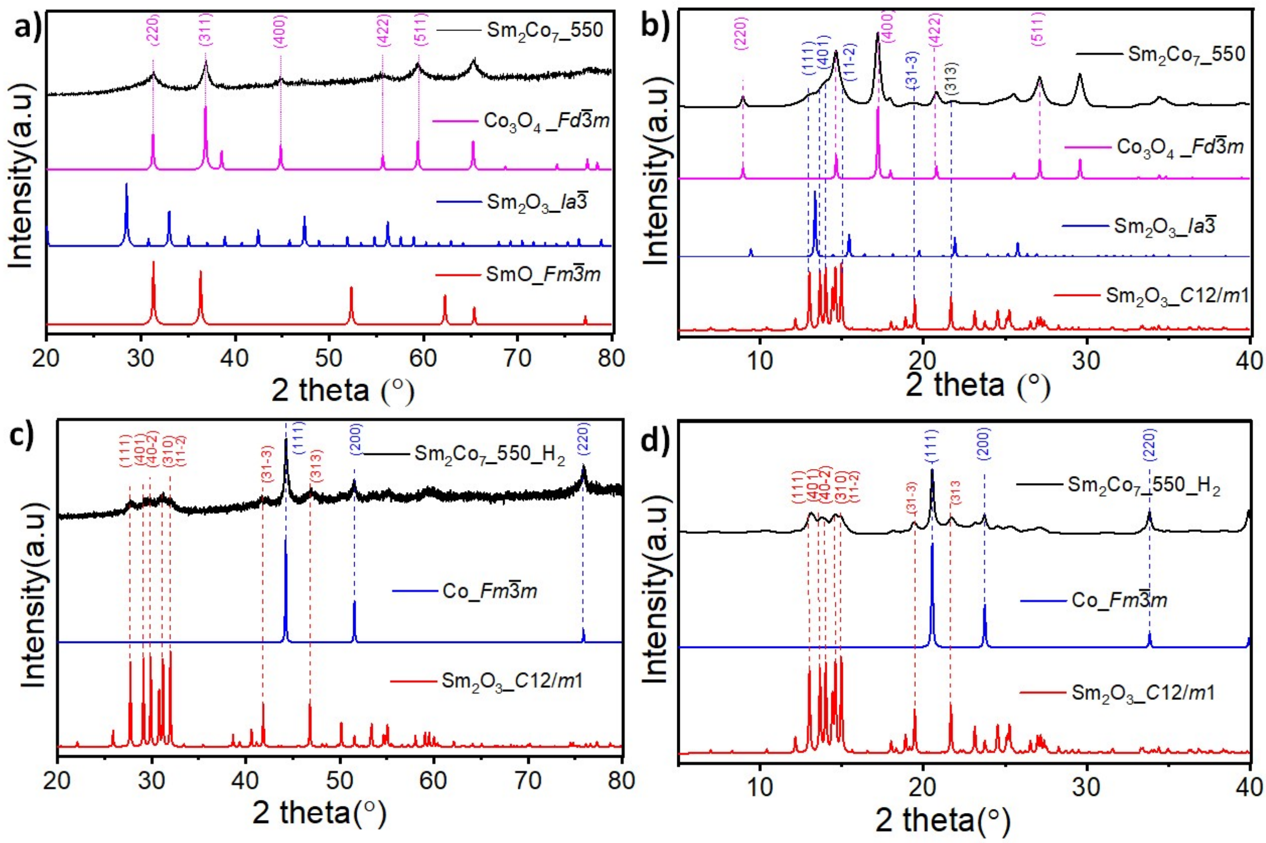

Figure S2. . Comparison of low and high energy XRD patterns of Sm_2Co_7_550 (a&b) and Sm_2Co_7_550_H_2 (c&d).

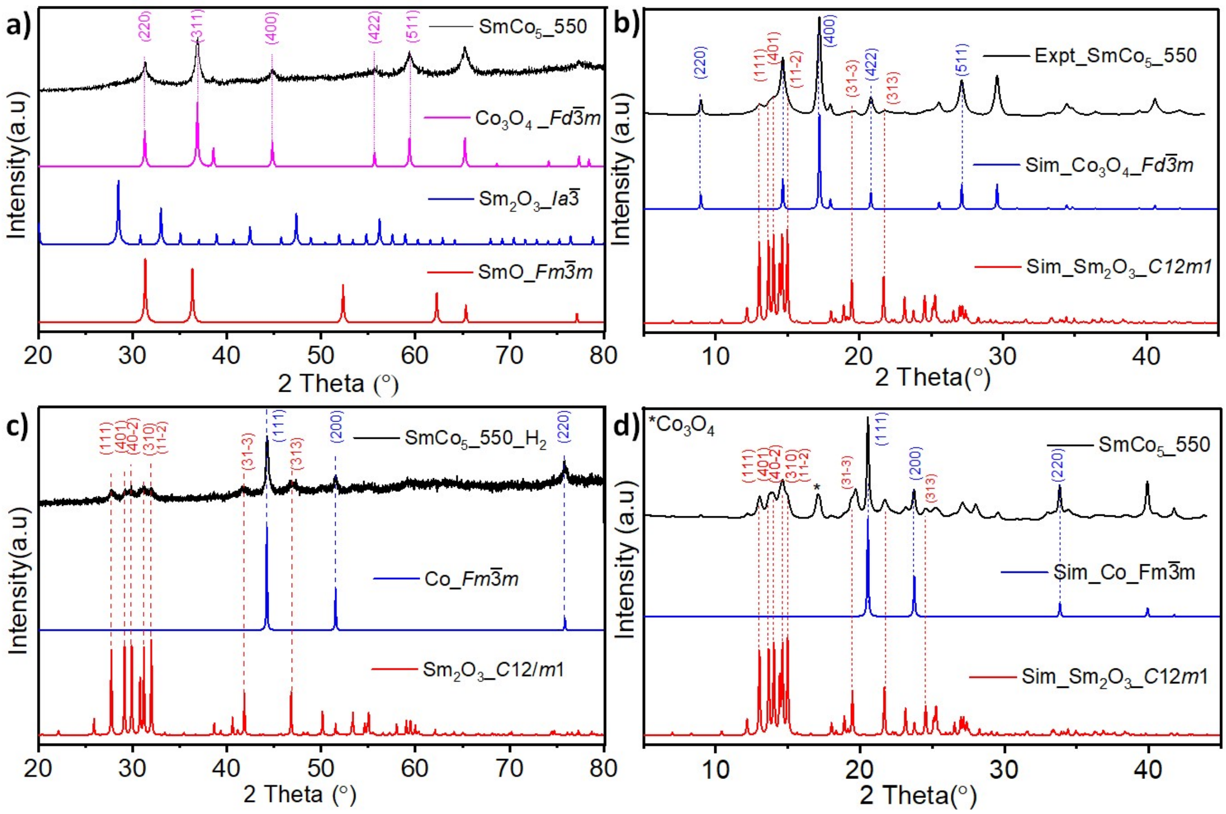

Figure S3. Comparison of low and high energy XRD patterns of $SmCo_5$_550 (a&b) and $SmCo_5$_550_H_2 (c&d).

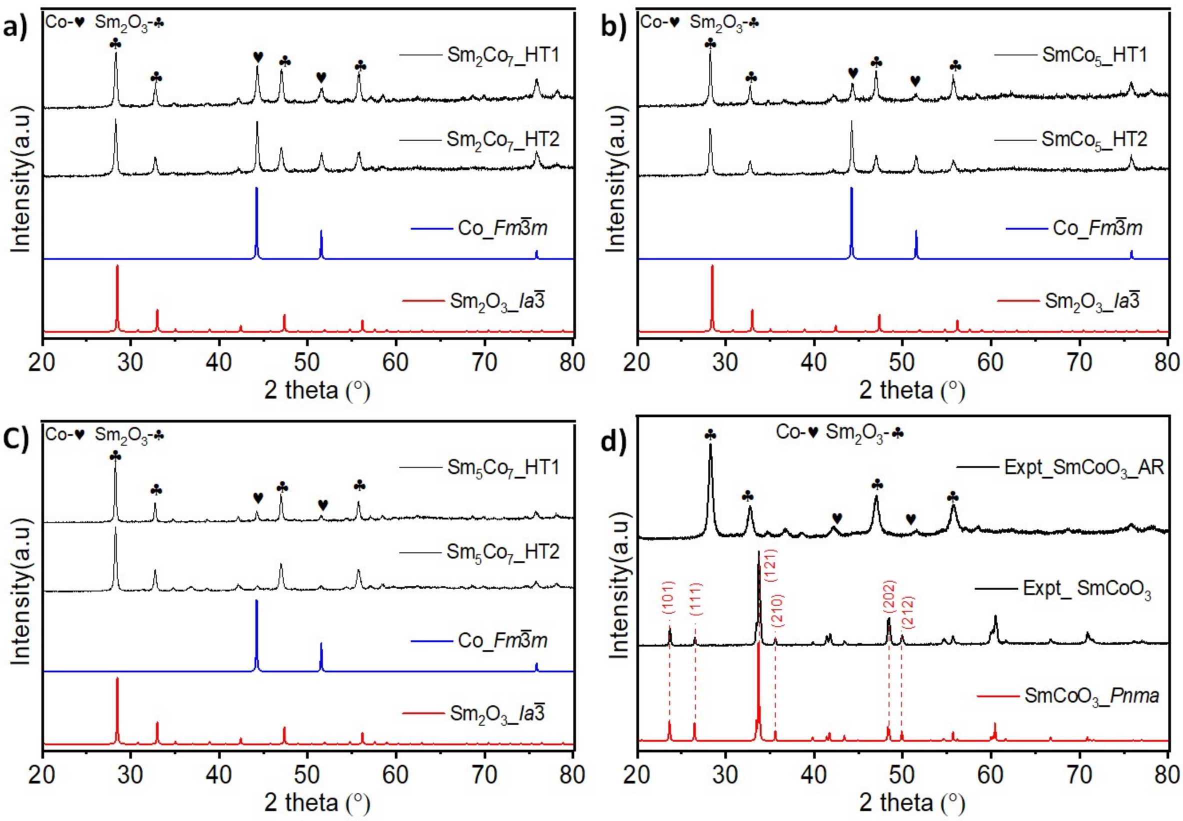

Figure S4. XRD pattern a) Sm_2Co_7 b) $SmCo_5$ c) Sm_5Co_7 compounds synthesized by HT1 and HT2 hydrothermal methods. d) Comparison of XRD patterns of $SmCoO_3$ with simulated one before reaction and after reaction (AR).

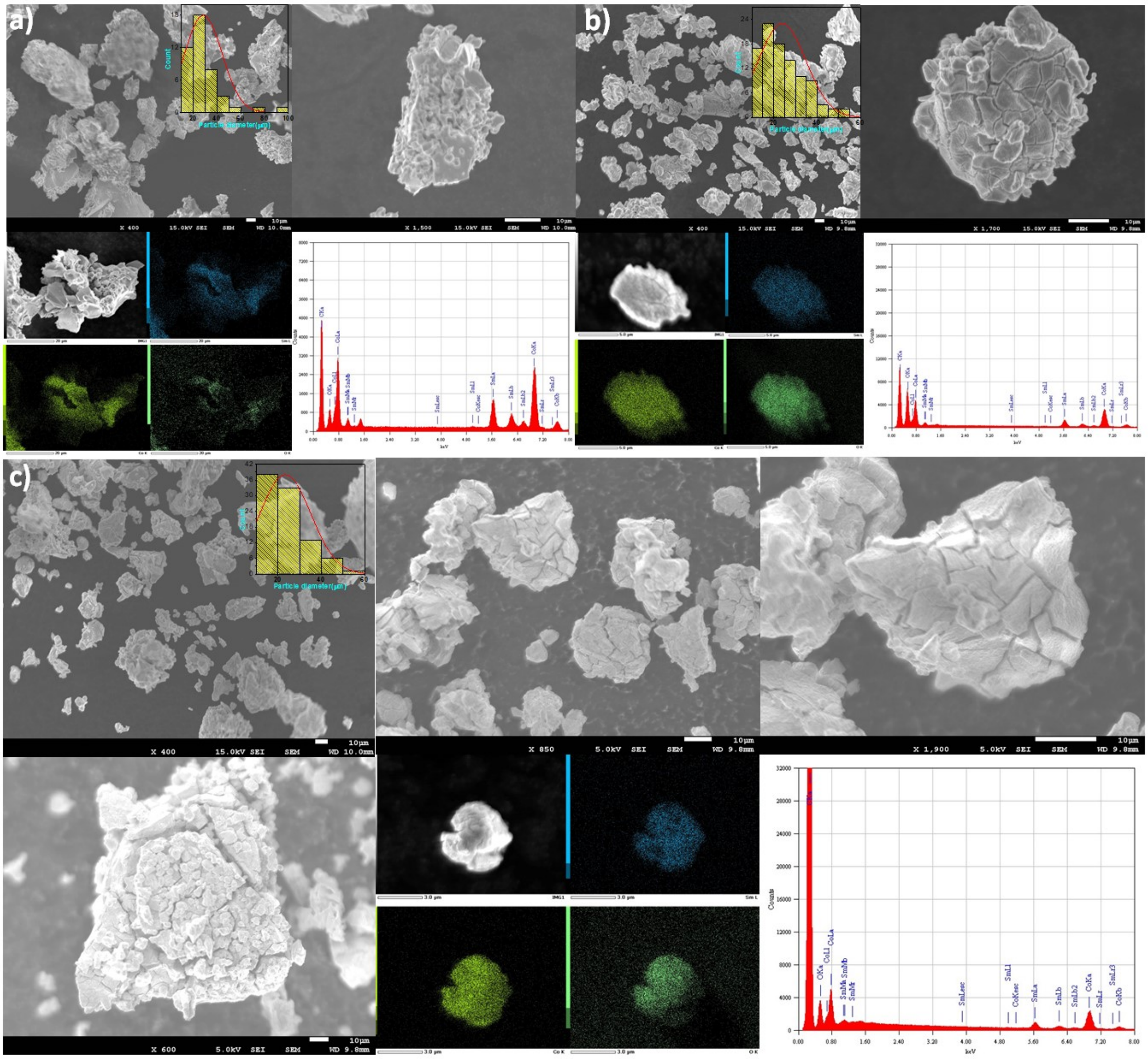

Figure S5. SEM images, particle size distribution, color mapping (Blue-Sm, Yellow, Co, Green -O) and EDAX spectra of a) $SmCo_5$ b) $SmCo_5$_550, and c) $SmCo_5$_550_H_2.

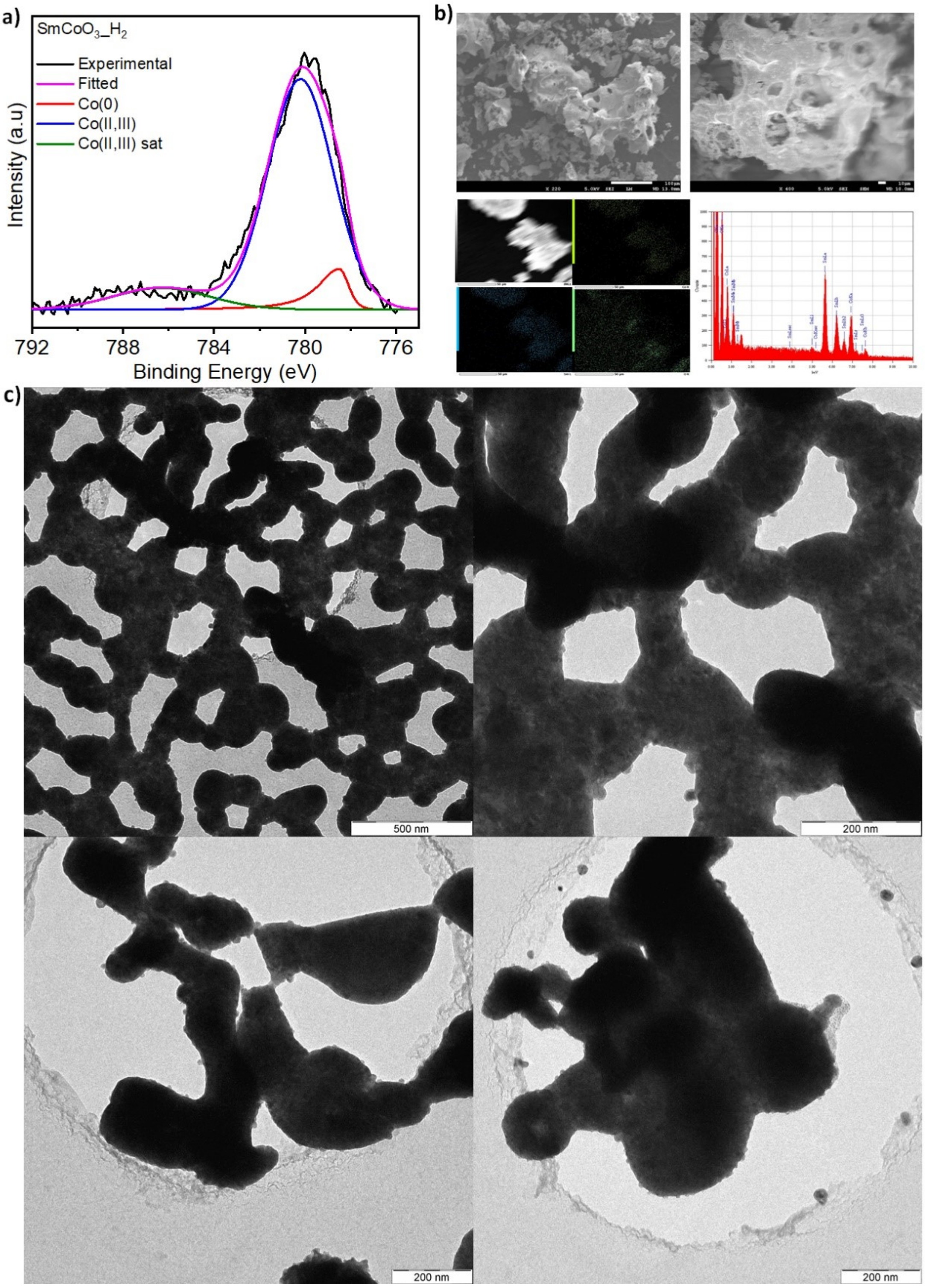

Figure S6. a) Co $2p_{3/2}$ XPS spectra, b) SEMand c) TEM images of $SmCoO_3\_H_2$

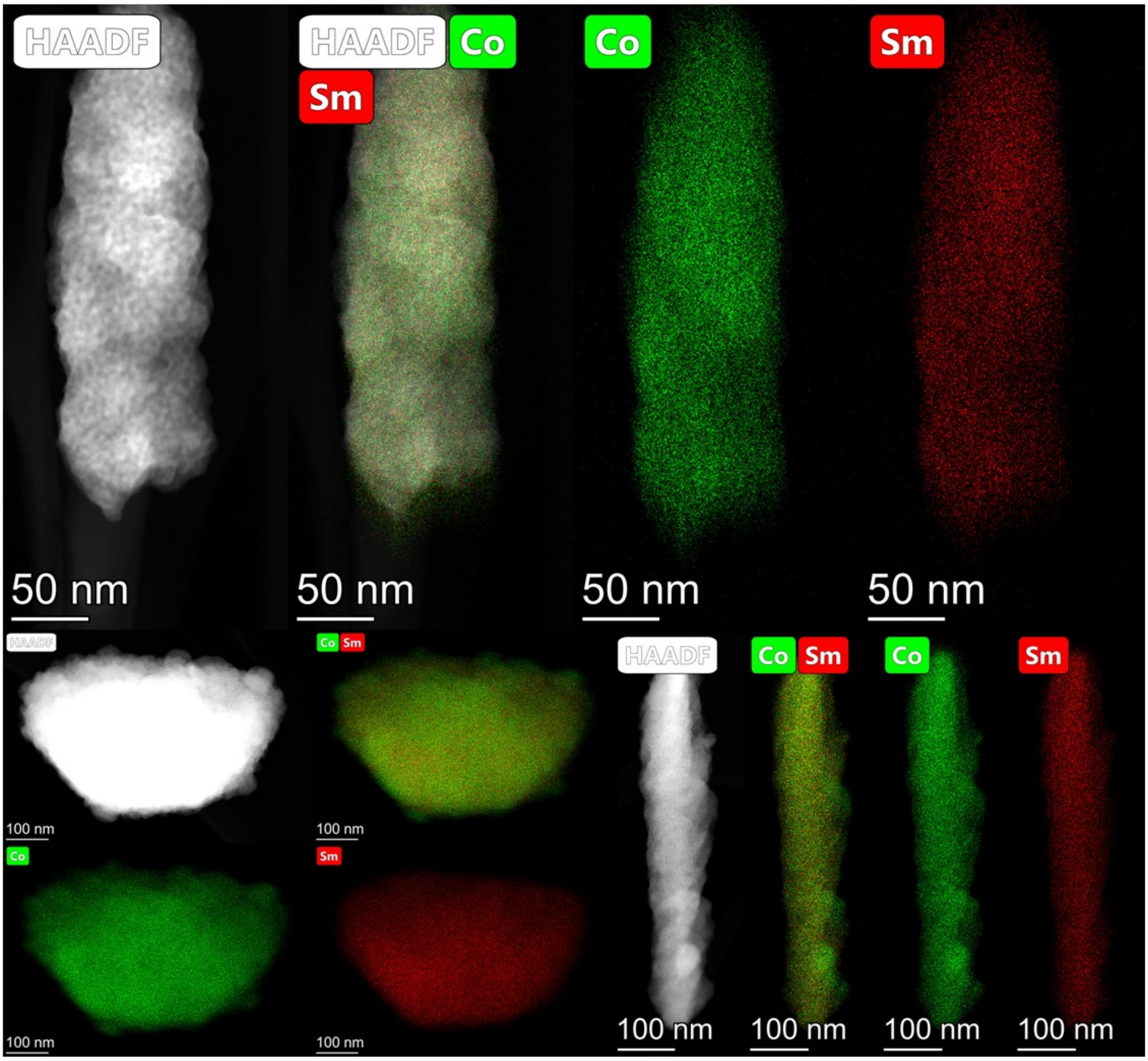

Figure S7. HAADF-STEM images and elemental color mapping of Sm_2Co_7_550

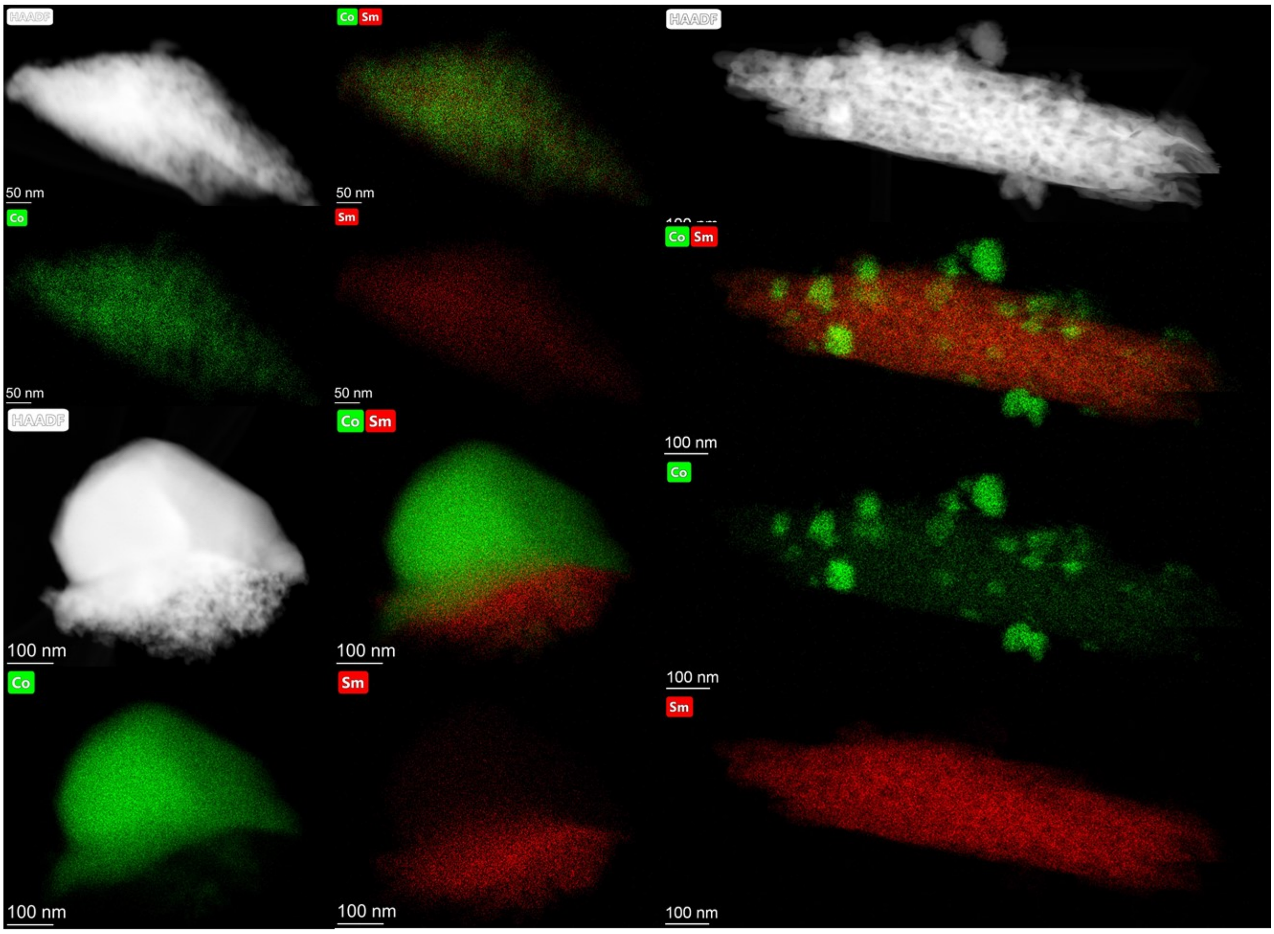

Figure S8. HAADF-STEM images and elemental color mapping of Sm_2Co_7_550_H_2

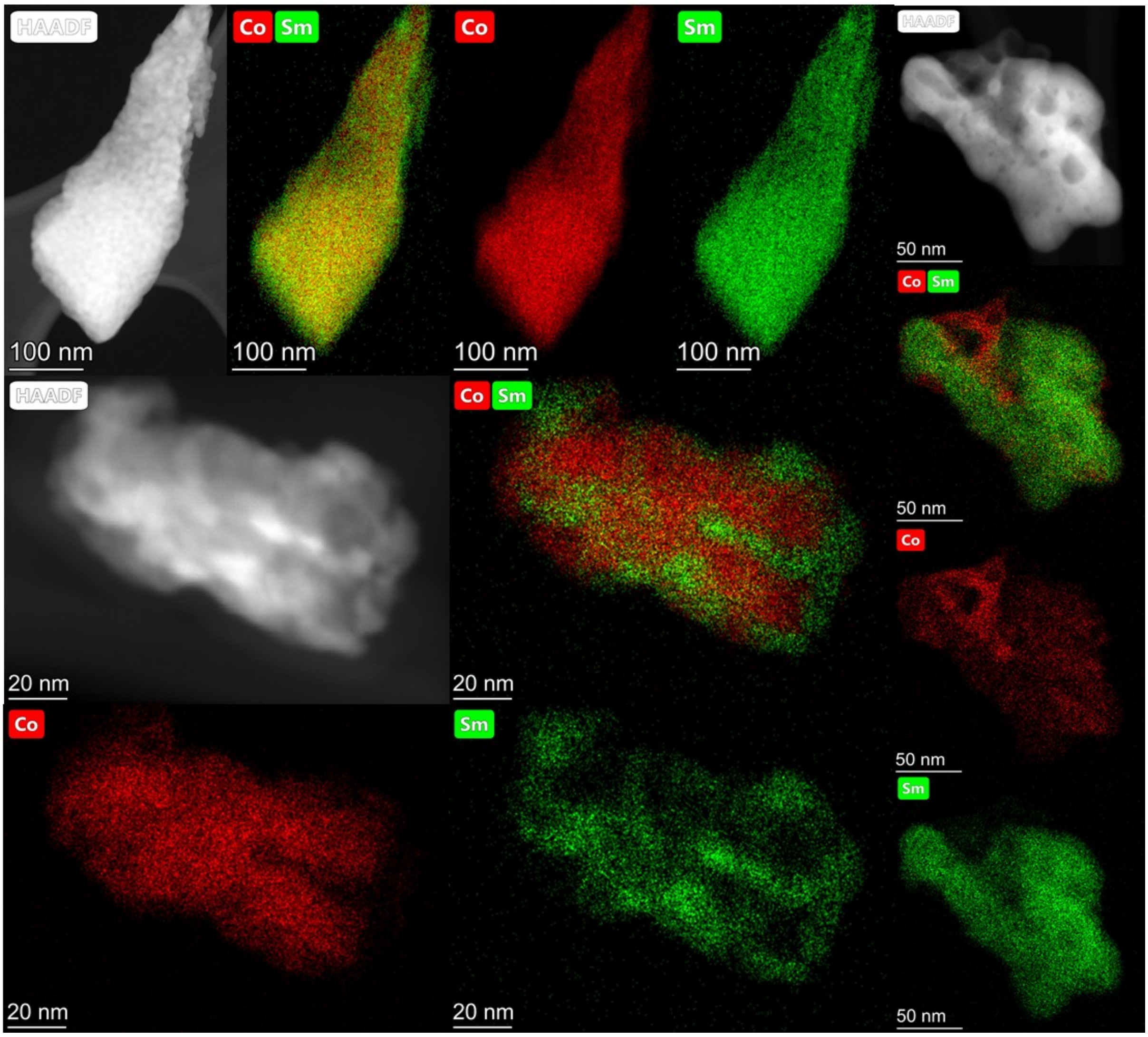

Figure S9. HAADF-STEM images and elemental color mapping of $SmCo_5$_550_H_2

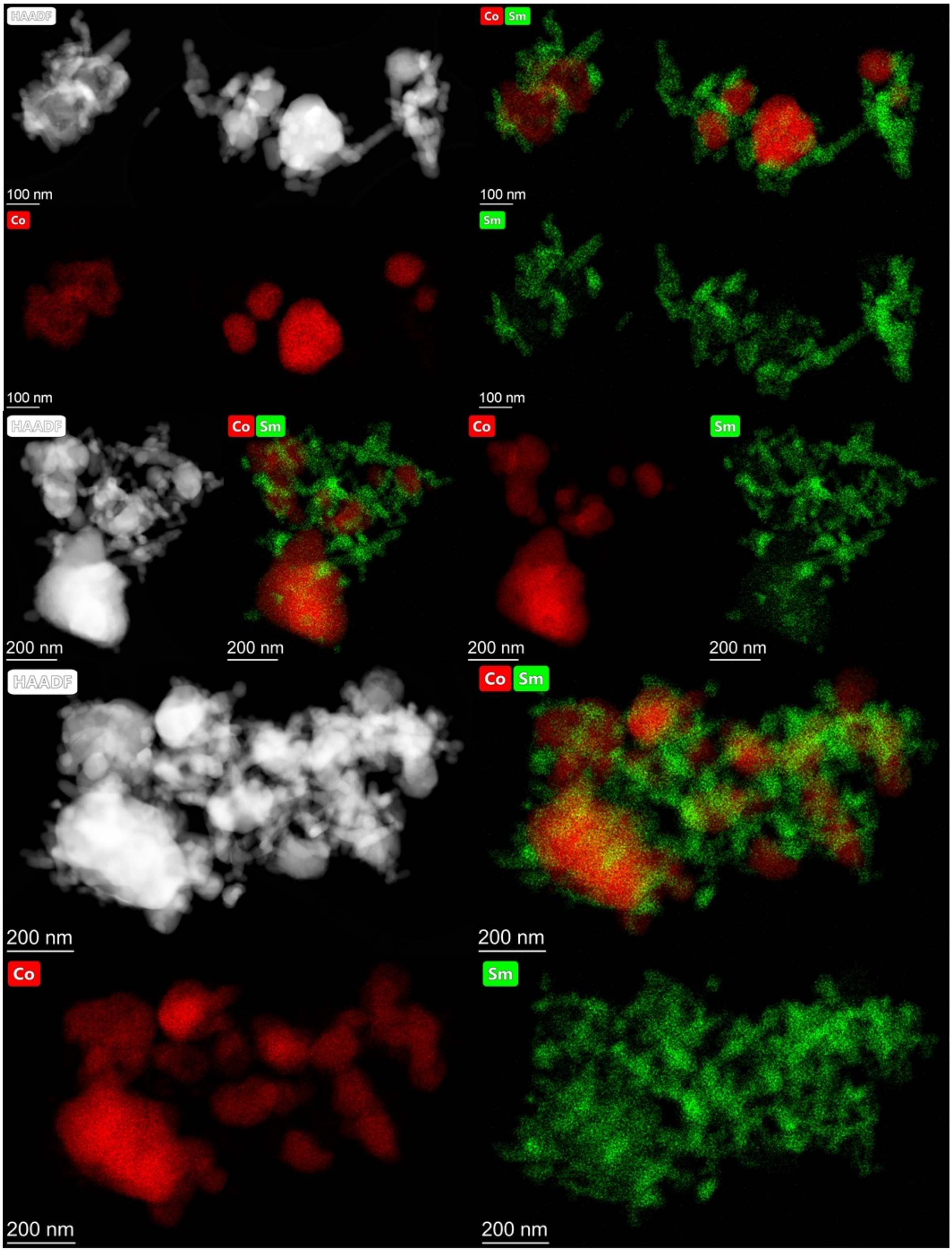

Figure S10. HAADF-STEM images and elemental color mapping of $SmCo_5$_HT2.

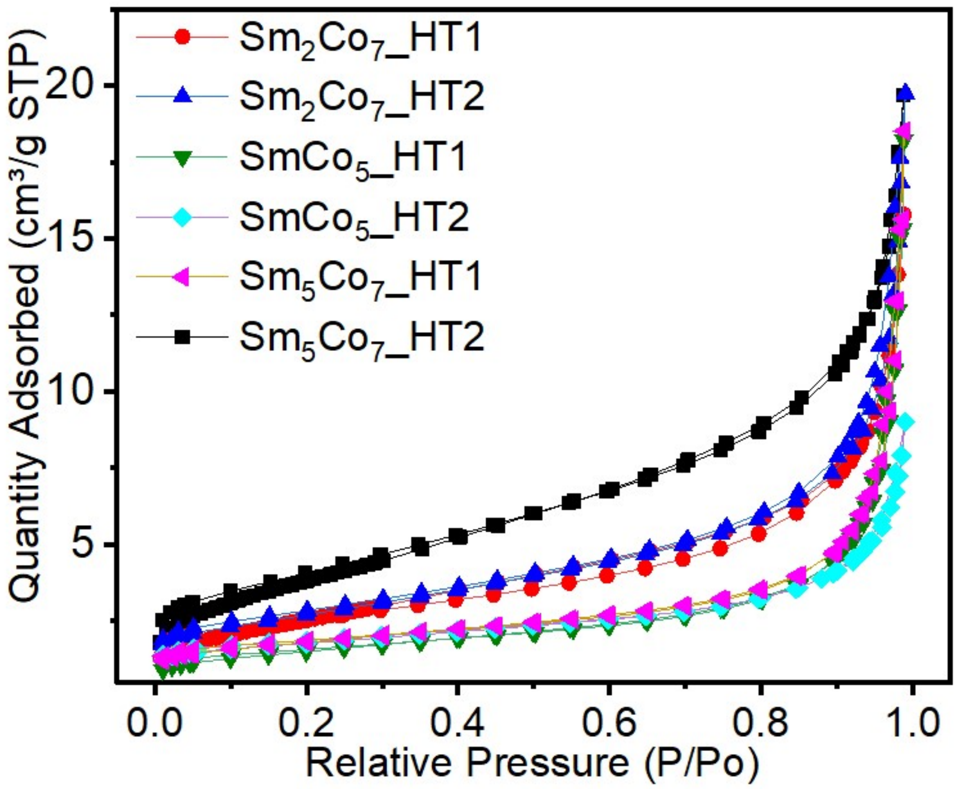

Figure S11. N_2 adsorption-desorption isotherms of Sm_xCo_y catalysts synthesized from hydrothermal method.

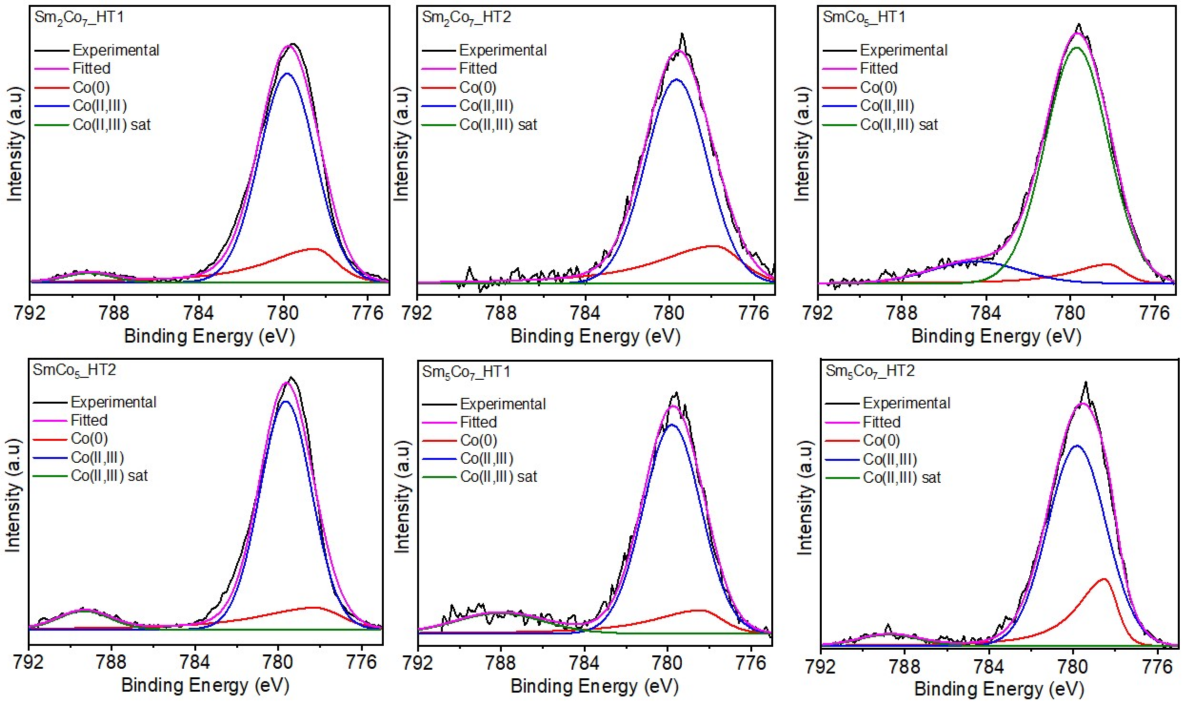

Figure S12. XPS of all the Co/Sm_2O_3 catalysts synthesized by hydrothermal method.

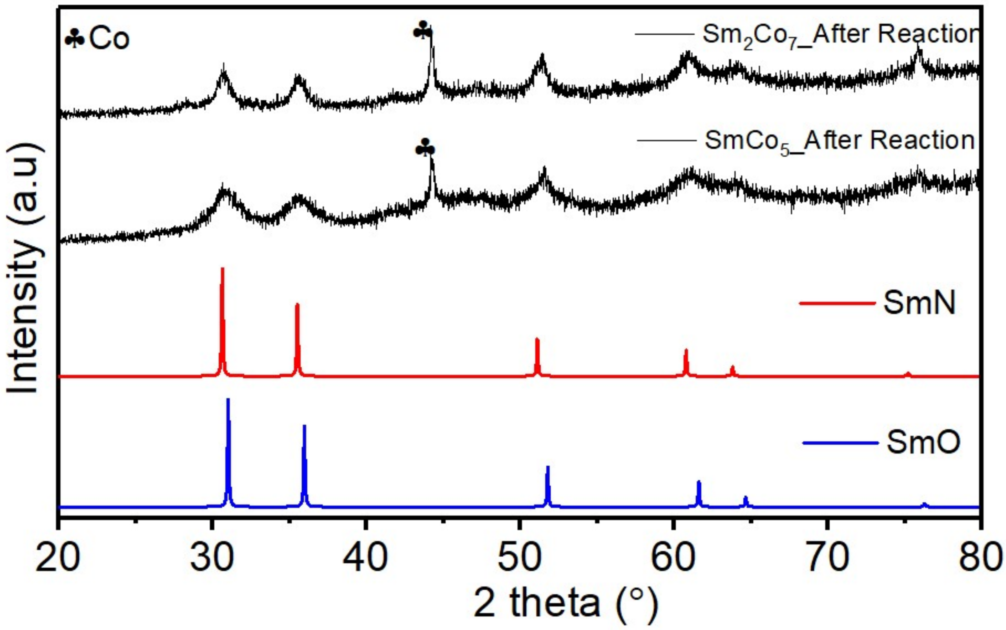

Figure S13. Comparison of XRD patterns of Sm_2Co_7 and $SmCo_5$ after reaction with simulated SmO and SmN.

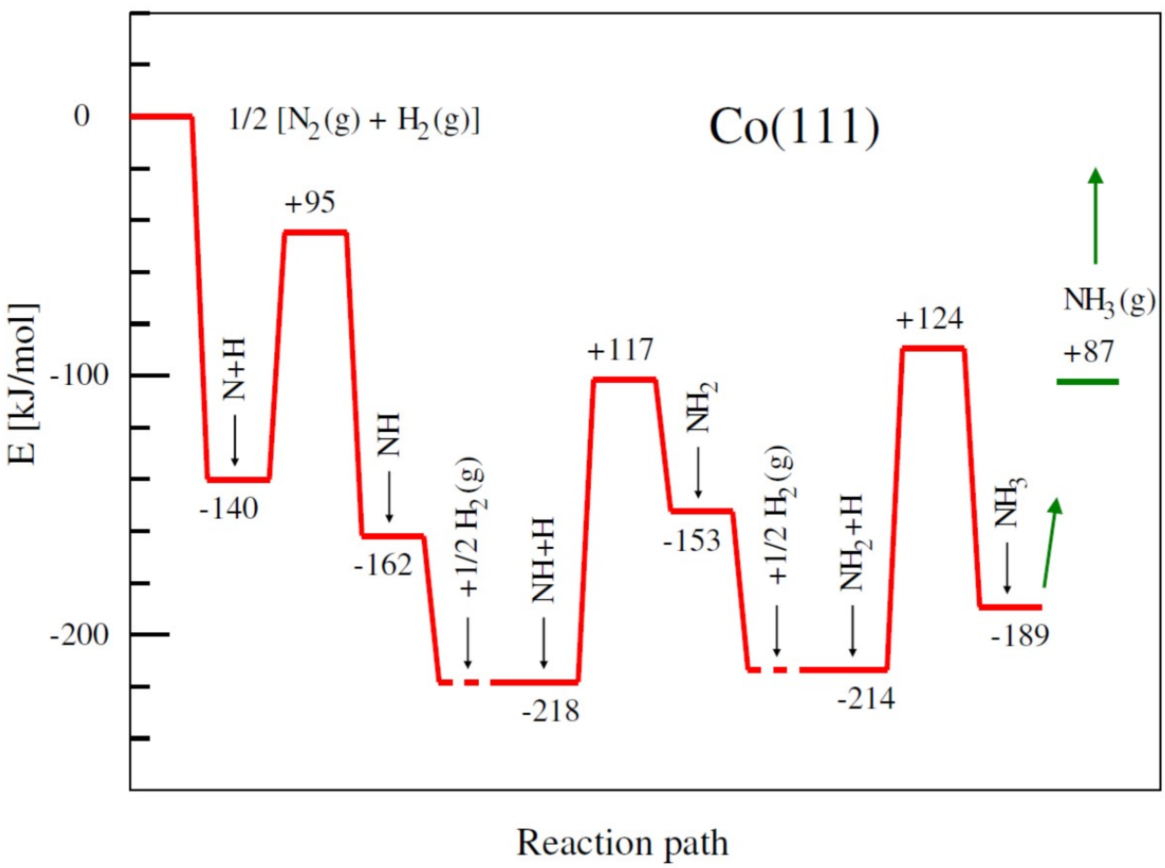

Figure S14. Energy profile of hydrogenation steps of NH_3 synthesis on the Co(111) surface**.**

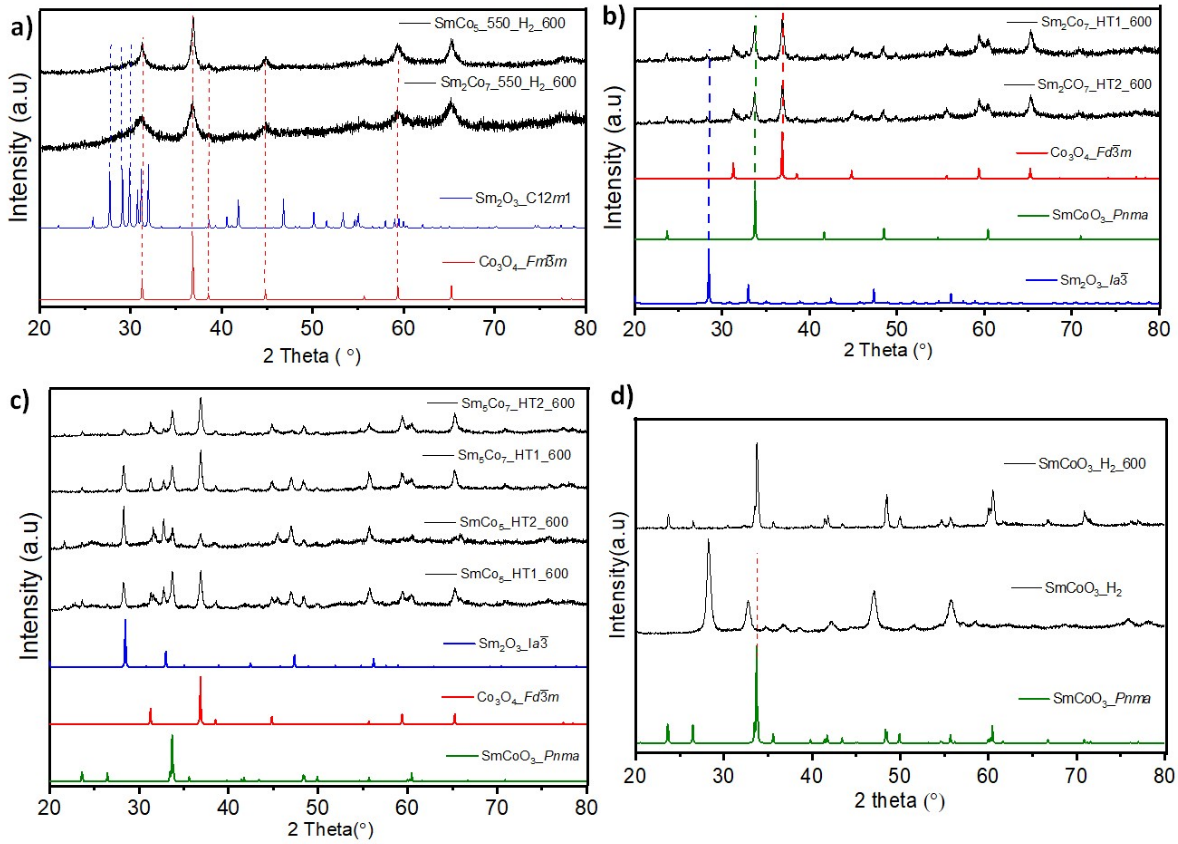

Figure S15. XRD patterns of all the Co/Sm_2O_3 after oxidation at 600 °C a) IMC derived, b&c) hydrothermally synthesized and d) Perovskite derived. In case of all the HT catalysts a small amount of $SmCoO_3$ is formed along with Co_3O_4/Sm_2O_3, but for IMC derived catalysts only Co_3O_4/Sm_2O_3 phase is observed instead. For perovskite derived Co/Sm_2O_3 catalyst the perovskite structure is completely restored.

Table S1. Crystalite size of Sm_xCo_y catalysts calculated using the Scherrer equation.

Entry	Catalysts	Crystallite Size(nm)			
		Intermetallic	Sm_2O_3	Co_3O_4	Co
1	Sm_2Co_7	34	--	--	--
2	Sm_2Co_7_550	--	5*	11	
3	Sm_2Co_7_550_H_2	--	10*	--	19
4	$SmCo_5$	29	--	--	--
5	$SmCo_5$_550	--	11*	13	
6	$SmCo_5$_550_H_2	--	15*	--	23
7	Sm_2Co_7_550_HT1	--	26	--	25
8	Sm_2Co_7_550_HT2	--	17	--	23
9	$SmCo_5$_550_HT1	--	22	--	19
10	$SmCo_5$_550_HT2	--	24	--	30
11	Sm_5Co_7_550_HT1	--	27	--	25
12	Sm_5Co_7_550_HT2	--	23	--	12
13	$SmCoO_3$_550	--	19	--	--

*determined by high energy synchrotron XRD.

Catalysts	T_α	T_β	T_γ
Sm_2Co_7_550	361	417	471
$SmCo_5$_550	346	394	446
Sm_2Co_7_550_HT1	318	365	418
Sm_2Co_7_550_HT2	328	401	472
$SmCo_5$_550_HT1	319	366	401
$SmCo_5$_550_HT2	320	358	399
Sm_5Co_7_550_HT1	340	432	502
Sm_5Co_7_550_HT2	355	437	496

Table S2. Fitted components of TPR-H_2 spectra of Sm_xCo_y catalysts.

Table S3. Comparison of catalytic activity of the Co/Sm_2O_3 catalyst with other reported cobalt-based catalysts

Entry	Catalyst	Surface Area [m² /g]	Temperature [°C]	Pressure [MPa]	NH_3 yield [µmole/g/h]	Ea [kJ/mole]	Ref
1	Co-LiH	42	300	1	4800	52.1	[24]
2	Co-BaH2/CNT	53	300	1	4800	58.0	[25]
3	Co/$BaTiO_{2.35}H_{065}$	05	400	5	550	69.0	[50]
4	Co/C12A7:e^-	01	340	0.1	912	49.5	[26]
5	LaCoSi	01	400	0.1	1250	42.0	[51]
6	Co_3Mo_3N	18	400	0.1	489	59.0	[51]
7	Co/CeO_2-dopamine	61	425	1	19200	72.0	[22]
8	Co/CeO_2	60	425	1	3810	107	[22]
9	$LaCoO_3$	05	450	1	4600	--	[33]
10	Sm_2Co_7_550_H_2	13	350	0.4	250	77.0	Present work
			400	0.4	500		
			450	0.4	1600		
			500	0.4	3850		
11	Co/SmO	01	350	0.4	150	52.0	Present work
			400	0.4	300		
			450	0.4	550		
			500	0.4	1000		